High Energy Nucleus-Nucleus Collisions In View Of The Multi-Peripheral Model

M. T. Hussein and N. M. Hassan and * N. Elharby

Physics Department, Faculty of Science, Cairo University, Cairo - Egypt
* Physics Department, Faculty of Education for Girls, Jeddah, KSA.

Abstract. The hypothesis of the multi peripheral model is extended to the hadron-nucleus interactions and then generalized to the nucleus-nucleus case. The processing of the model depends on input parameters that are extracted from the features of the experiments in this field. The number of encountered nucleons from both target and projectile are estimated according to the eikonal scattering approach. The screening effect due to the interaction of the projectile nucleons in successive manner with the target nucleus is considered. The rapidity distributions of fast particles are reproduced for the successive collisions in p-S and ^{32}S-^{32}S interactions at 200 A GeV. A global fair agreement is found in comparison with data of the experiment SLAC-NA-035.

PACS numbers: 05.70.Cd

1. Introduction

In the last few years the research work was concentrated on possible existence of the quark-gluon plasma phase, considering of unconfined quarks and gluons at high temperature or high density. In the laboratory, nucleus-nucleus collisions at very high energies provide a promising way to produce high temperature or high-density matter. As estimated by Bajorken [1] the energy density can be so high that these reactions might be utilized to explore the existence of the quark-gluon plasma. One of the many factors that lead to an optimistic assessment that matter at high density and high temperature may be produced with nucleus-nucleus collisions is the occurrence of multiple collisions. By this mean, a nucleon of one nucleus may collide with many nucleons in the other and deposits a large amount of energy in the collision region. In the nucleon-nucleon center of mass system, the longitudinal inter-nucleon spacing between target nucleons are Lorentz contracted and can be smaller than 1 fm in high-energy collisions. On the other hand, particle production occurs only when a minimum distance of about 1 fm separates the leading quark and antiquark in the nucleon-nucleon center of mass system [2,3]. Therefore when the projectile nucleon collides with many target nucleons, particles production arising from the first N-N collision is not finished before the collision of the projectile with another target nucleon begins. There are models [4-11] that describe how is the second collision is affected by the first one. Nevertheless, the fundamental theory of doing that remains one of the unsolved problems. Experimental data suggest that after the projectile nucleon makes a collision, the projectile-like object that emerges from the first collision appears to continue to collide with other nucleons in the target nucleus on its way through the target nucleus. In each collision the object that emerges along the projectile nucleon direction has a net baryon number of unity because of the conservation of the baryon number. One can speak loosely of this object as the projectile or baryon-like object and can describe the multiple collision process in terms of the projectile nucleon making many collisions with the target nucleons. Then, losing energy and momentum in the process, and emerging from the other side of the target with a much diminished energy. The number of collisions depends on the thickness of the target nucleus. Experimental evidence of occurrence of multiple collision process can be best illustrated with the data of p-A reactions in the projectile fragmentation region [3, 12]. In the present work we shall investigate the particle production mechanism in heavy ion collision by extending the multi-peripheral model [13-15] to the nucleon-Nucleus and then generalize to the nucleus-nucleus case. The paper is organized so that in section **2**, we present the experimental features of high-energy events. This will serve in setting the boundary condition of the extended problem and building up the model in a realistic form. The hypothesis of the multi-peripheral model is demonstrated in section **3**. The nucleon-nucleon case is briefly described in **3.1** and the extension to the nucleon-nucleus and the nucleus-nucleus collisions are followed in section **3.2** and **3.3** respectively. Concluding remarks are given in section **4**.

2. Experimental Features of High Energy Events

The heavy ion collisions initiate the chance of processing multiple collisions of single nucleon-nucleon (N-N) events. This behavior allows the magnification of any small signal that may appear unclear in (N-N) event. The magnification increases as the size of the interacting nuclei increases. Nevertheless, the relation is not simply linear but many other factors are expected to contribute the complexity of the problem. The study of the multiplicity distribution at different rapidity intervals carries valuable information in this sense [16]. The rapidity range is classified into regions that characterizes the type of the interaction. The target and the projectile fragmentation regions contain the fast particles characterizing the forward and backward production from the fragmentation of both the target and the projectile nuclei in their center of mass system. The central rapidity interval is the hot region of the reaction. It sends global information about the strong interactions inside the nuclear bowl. Moreover, signals about (QGP) may be extracted from the study of this region. Fig. (1) shows the experimental data of the rapidity distributions of fast particles produced in the interaction of sulfur-projectile with proton, sulfur, silver and gold as target nuclei at 200 A GeV incident energy [17]. The average multiplicity at each rapidity interval depends on the incident projectile energy (which is fixed in this case) and the size of the interacting nuclei. The nucleus-nucleus (A-A) collision may be seen as N-N base or N-A base. To put the problem in a quantitative measurable form, we define a multiplication factor *MF (N_N)* as a base of (N-N);

$$MF_{(N-N)} = \frac{Yield, in(A-A)}{Yield, in(N-N)} \tag{1}$$

And the multiplication factor MF (N-A) as a base of (N-A);

$$MF_{(N-A)} = \frac{Yield, in(A-A)}{Yield, in(N-A)} \tag{2}$$

Fig. (2) and Fig. (3) show the multiplication factors based on (N-N) and (N-A) for the different reactions. The multiplication factor has maximum value at the central rapidity region (Y˜0) in both cases. The experimental data of p-S and the S-S collisions show constant value allover the rapidity range. Nevertheless, it is difficult to estimate the number of base-collisions in each reaction from this approach. An alternative approach is to renormalize the rapidity distribution to get a scaled function that is independent on the projectile and target size. The average number of encountered nucleons from the target by an incident hadron [16,18] is a good measure of the number of collisions inside a target nucleus. This is defined as,

$$\nu = A_t \frac{\sigma_{hN}}{\sigma_{hA}} \tag{3}$$

Where σ_{hN}, and σ_{hA} are the total inelastic cross section of (h-N) and (N-A) respectively. By analogy, the average number of binary (N-N) collisions inside the

(A-A) collision may be defined as,

$$\nu_{NN} = A_p A_t \frac{\sigma_{hN}}{\sigma_{AA}} \tag{4}$$

σ_{AA} is the total inelastic cross section of (A-A) collision at the same incident energy. On the other hand, the average number of collisions based to N-A is defined as,

$$\nu_{NA} = A_p \frac{\sigma_{hAt}}{\sigma_{AA}} \tag{5}$$

is total inelastic cross section of (h-At) collision. The scaling function is then obtained by dividing the rapidity distribution by the average number of collisions or . The resultant are displayed in Fig. (4) which shows the overlapped distributions corresponding to the reactions of different nuclear sizes. Following now a geometric approach which assumes that the nuclear radius is linearly proportional to the one third power of its mass number, then Eqs.(3-5) becomes,

$$\begin{aligned} \nu &= A_t^{1/3} \\ \nu_{NN} &= \frac{A_p A_t}{A_t^{2/3} + A_p^{2/3} + 2A_t^{1/3} A_p^{1/3}} \\ \nu_{NA} &= \frac{A_p A_t^{2/3}}{A_t^{2/3} + A_p^{2/3} + 2A_t^{1/3} A_p^{1/3}} \end{aligned} \tag{6}$$

Let $\overline{m}$ be the average multiplicity produced in N-N collision and $\overline{m}_{NA}$ is the corresponding figure for N-A collision at the same incident energy. So that the average multiplicity produced in A-A collisions may be calculated in base of N-N as,

$$\overline{m}_{AA} = \nu_{NN} \overline{m} \tag{7}$$

and in base of N-A as,

$$\overline{m}_{AA} = \nu_{NA} \overline{m}_{NA} \tag{8}$$

Table (1) shows the values of $\overline{m}_{AA}$ as calculated by Eqs.(7 & 8) compared with the experimental data. The comparison of the last three columns shows that the predicted values of $\overline{m}\nu_{NN}$ are more close to the experimental data which implies that the A-A collision behaves as a base of N-N not N-A collision.

Table (1)

Reaction	ν_{NN}	ν_{NA}	$\overline{m}\ \nu_{NN}$	$\overline{m}_{NA}\ \nu_{NA}$	$\overline{m}_{AA}$(exp)
p-S	1.83	0.25	5.87	1.48	5.90
p-Au	4.20	0.42	13.5	4.14	9.90
d-Au	7.8	0.83	25.2	11.3	23.0
O-Au	45.3	6.70	145.0	90.0	137.0
S-S	25.4	8.0	81.3	47.2	90.0
S-Ag	54.8	27.0	175.0	160.0	162.0
S-Au	77.9	49.2	250.0	290.0	225.0

3. The Multi-Peripheral Model

3.1. Hadron-Nucleon Collision

The multi-peripheral technique was found to be a good tool in dealing with the problems of multi particle production [13,14] in hadron proton (h-p) interactions. In this technique, the many body-system is expanded into subsystems, each concerns a two body collision. It is assumed that each hadron in the final state is produced at a specific peripheral surface that is characterized by a peripheral parameter. The phase space integral $I_n(s)$ of the produced hadrons is a measure of the probability of producing n particle in the final state at center of mass energy $\sqrt{s}$. It depends mainly on the volume in phase space and the transition matrix element T, and defined as,

$$I_n(s) = \int \cdots \int \prod_i^n \frac{d^3p_i}{2E_i} \delta^4(\sqrt{s} - \sum_j p_j)|T|^2 \tag{9}$$

Eq. (9) may be simplified as if expressed as a sequence of two particle decay Fig.(5). Accordingly, the integration in Eq. (9) becomes,

$$I_n(s) = \int_{\mu_{n-1}^2}^{(M_n - m_n)^2} dM_{n-1}^2 I_2(k_n^2, k_{n-1}^2, p_n^2) I_{n-1}(M_{n-1}^2)|T|^2 \tag{10}$$

$$= \int_{\mu_{n-1}^2}^{(M_n - m_n)^2} dM_{n-1}^2 \int d\Omega_{n-1} \frac{\lambda^{1/2}(M_n^2, M_{n-1}^2, m_n^2}{8M_n^2} \; I_{n-1}(M_{n-1}^2)|T|^2$$

Where M_i is the invariant mass of the subsystem composed of $i-$particles. The integration over all possible values of M_{n-1} concerns the first vertex in the chain of Fig.(5). To proceed further, we iterate Eq.(10) for the M_{n-2}, M_{n-3}, M_2 to obtain the entire chain, so that,

$$I_n(s) = \int_{\mu_{n-1}}^{(M_n - m_n)} dM_{n-1} d\Omega_{n-1} \frac{1}{2} P_{n-1}|T(P_{n-1})|^2 \cdots \int_{\mu_2}^{(M_3 - m_3)} dM_2 d\Omega_2 \frac{1}{2} P_3 |T(P_2)|^2$$

$$\cdot \int d\Omega_1 \frac{1}{2} P_2 |T(P_1)|^2 \tag{11}$$

Where $P_i = \lambda^{1/2}(M_i^2, M_{i-1}^2, m_i^2)$ is the three-vector momentum of the ith particle and $T(p_i)$ is the transition matrix element at the ith vertex. For the case of strong interactions $T(p_i)$ has a parametric form which cut the magnitude of the particles momenta according to their physical region [16,19],

$$T(p_i) = \exp(-\alpha_i p_i) \tag{12}$$

And α_i is a peripheral parameter, which fits the experimental data. The multiple integration in Eq. (11) may be solved by the Monte Carlo technique [20-22]. At extremely high energy, Eq. (11) has an asymptotic limit in the form;

$$I_n(s) = \frac{(\pi/2)^{n-1}}{(n-1)!(n-2)!} s^{n-2} |T|^{2(n-1)} \tag{13}$$

3.2. Hadron-Nucleus Collisions

On extending the model to the hadron-nucleus or nucleus-nucleus collisions, we follow the NN-base super position as expected from the features of the experimental data that are illustrated in section **2**. We should consider the possible interactions with the nucleons forming the target nucleus A_t. The incident hadron makes successive collisions inside the target. The energy of the incident hadron (leading particle) slows down after each collision, producing number of created hadrons each time that depends on the available energy. The phase space integral I_n^{NA} in this case has the form,

$$I_n^{NA}(s) = \sum_{\nu}^{A_t} I_{n_\nu}(s_\nu) P(\nu, A_t) \delta(n - \sum_{i}^{A_t} n_i) \tag{14}$$

Where $P(\nu, A_t)$ is the probability that ν nucleons out of A_t will interact with the leading particle and $I_{n_\nu}(s_\nu)$ is the phase space integral of NN collision that produces hadrons at energy $\sqrt{s_\nu}$. The delta function in Eq.(14) is to conserve the number of particle in the final state. Treating all nucleons identically, and that X_{NN} is the $N-N$ phase shift function [18,23-25], then, according to the eikonal approximation,

$$P(l, A_t) = - \left(\begin{array}{c} A_t \\ l \end{array} \right) \sum_{j=0}^{l} (-1)^j \left(\begin{array}{c} l \\ j \end{array} \right) \{1 - \exp(2Rei(A_t - l + j) X_{NN})\} \tag{15}$$

The working out of this approach is to put the multi-dimension integration of Eq. (11) and the generated kinematical variables into a Monte Carlo subroutine [16]. This in turn is restored ν times, where ν is the number of collisions inside the target nucleus that is generated by a Monte Carlo Generator according to the probability distribution Eq.(15). In the first one, the incident hadron has its own incident energy E_0 and moves parallel to the collision axis (z-axis) $\theta_0 = 0$. The output of the subroutine determines the number of created hadrons n1 as well as the energy $E_1 (< E_0)$ and the direction q1 of the leading particle. The leading particle leads the reaction in its second round with E_1 and θ_1 as input parameters and creates new number of particles $n-2$ and so on. The number nj is determined according to a multiplicity generator which depends on the square of the center of mass energy sj in the round number j.

$$s_j = 2m_N^2 + 2m_N E_j \tag{16}$$

Fig. (6) demonstrates the particle rapidity distribution produced in the first three-collisions as predicted by the model for the p- ^{32}S at 200 GeV. The yield (as measured by the area under the curve) decreases with the order of the collision because of the appreciable drop in the energy after the successive collisions. On the other hand, the family of curves concerning the different number of collisions acquires gradually decreased rapidity range. The overall distribution is compared with the experimental data SLAC-NA-035 in Fig. (7). The comparison shows good agreement.

3.3. Nucleus-Nucleus Collisions

The extension of the multi peripheral model to the nucleus- nucleus case is more complicated. The number of available collisions is multi-folded due to the contribution of the projectile nucleons. By analogy to the N-A collision, it is possible to define the phase space integral I_n^{AA} in $A-A$ collisions as,

$$I_n^{AA}(s) = \sum_{j}^{A_p} \sum_{k}^{A_t} I_{n_{j,k}}(s_{j,k}) P_{AA}(j, A_p, k, A_t) \delta(n - \sum_{j,k}^{A_t} n_{j,k}) \tag{17}$$

Where $I_{n_{j,k}}(s_{j,k})$ is the phase space integral due to the knocked on nucleon number j from the projectile and that, number k from the target. The probability that the $A-A$ collision encounters ν_p collisions from the projectile and ν_t collisions from the target is treated as independent events. So that,

$$P_{AA}(j, A_p, k, A_t) = P(\nu_p, A_p) \cdot P(\nu_t, A_t) \tag{18}$$

Another modification is carried out on this calculation that is to consider the screening effect of the projectile nucleons upon the interaction. This effect is summarized as follows. The first projectile nucleon faces the target nucleus as a whole, i.e. it can see the complete A_t nucleons and interacts with only ν_{t1} of them. The next projectile nucleon will see that target as partially screened by the first. The target size in this case is $A_t - \nu_{t1}$ and it interacts with only ν_{t2} nucleons according to a probability function, $P(\nu_{t2}, A_t - \nu_{t1})$, by simple iteration, the ith projectile nucleon will see a target as $A_t - \sum_k^{i-1} \nu_{tk}$and so on. The prediction of the model is applied to the ^{32}S-^{32}S collisions at 200 A GeV incident energy. The rapidity distribution of the produced particles in the first 3- projectile nock on nucleons is demonstrated in Fig. (8). While the overall rapidity distribution is compared with the data of the experiment SLAC-NA-035 in Fig. (9). The fair agreement obtained for $N-A$, Fig. (7) and $A-A$ collisions Fig. (9) supports the success of the multi-peripheral model. A small defect in the model for the NN case will be multi-folded and would be seen clearly in $N-A$ and $A-A$ collisions.

4. Summary and Conclusive Remarks

1- A scaling rapidity function is obtained for particles produced in h-N, $A-A$ and $A-A$ collisions, which assumes that the reaction is built on $N-N$ base.

2- The multi-peripheral model is extended to the nucleon-nucleus and the nucleus-nucleus interactions on bases of nucleon-nucleon collisions.

3- The phase space integral of the nucleon-nucleon collision is folded several times according to the number of encountered nucleons from the target.

4- The probability that ν nucleons from the target are encountered by a projectile nucleon is calculated in terms of the nucleon-nucleon phase shift according to the eikonal approximation.

5- The number of created particles in each collision is summed over to get the production in the nucleon-nucleus case, where the conservation of number of particles in the final state is taken into consideration.

6- In nucleus-nucleus collisions, we followed the statistics of independent events. The screening effect among the interacting projectile nucleons is also considered.

References

[1] J.D. Bajorken, Phys. Rev. D27 (1983) 140.
[2] W. Bosza and A Goldhaber, Phys. Lett. 139B (1984) 235
[3] A. Barton et al., Phys. Rev. D27, (1983) 2580.
[4] B. Anderson, G. Gustavson, and B. Nilsson-Almqvist, Nucl. Phys. B281 (1987) 289.
[5] B. Nilsson-Almqvist and E. Stenlund, Comp. Phys. Comm. 43 (1987) 387.
[6] H. Stocker, and W. Greiner, Phys. Lett. B243 (1990) 7.
[7] R. Matiello et al, Nucl. Phys. B24 (1991) 221.
[8] X.N. Wang and M. Gyulassy, Phys. Rev. D44, (1991) 3501.
[9] K. Geiger and B. Muller, Nucl. Phys. A544 (1992) 467.
[10] K. Geiger, Phys. Rev. D46 (1992) 4365.
[11] K. Geiger, Phys. Rev. D47 (1993) 133.
[12] A. Brenner et al, Phys. Rev. D20 (1982) 1497.
[13] M.T. Hussein, IC/92/166. Internal Report, ICTP, Trieste, Italy, - IL Nuovo Cimento 106 A (1993) 481.
[14] M.T. Hussein, N.M. Hassan and A. Rabea. IC/93/111, Internal Report, ICTP, Trieste, Italy. IL Nuovo Cimento 107 A (1994) 749
[15] M.T. Hussein, N.M. Hassan and A. Rabea, Particle World Vol. 4 No. 1 (1994) 4.
[16] M.T.Hussein, N.M. Hassan and M.A. Allam, Tr. J. Phys. 21, (1997) 241.
[17] T. Alber et al, Europe .Phys.J. C2, (1998) 643. - Direct communication with the particle data group (PDG) at Durham, England, Last updated at 1999.
[18] M.K. Hegab, M.T. Hussein and N.M. Hassan, Z. Physics A 336,(1990) 345
[19] M.T. Hussein, N.M. Hassan, M.K. Hegab, Can. J. Phys. 63 (1985) 1449-1452
[20] M.T. Hussein, Invited Talk, First International Conf. On Basic Science & Advanced Technology. Nov. 9 -12, 1996. Assiut, Egypt.
[21] M.T.Hussein, A. Rabea , A. El-Naghy and N.M. Hassan, Progress of Theoretical Phys. Japan. Vol. 93 No. 3 (1995) 585.
[22] N. M. Hassan, N. El-Harby and M. T. Hussein, hep-ph/9912412.
[23] E. Meggiolaro, Nucl. Phys. Proc. Suppl. 64 (1998) 191, hep-th/9709045
[24] F. Pereira, E. Ferreira, Phys. Rev. D59 (1999) 014008, hep-ph/9811496
[25] M. B. Gay Ducati, V. P. Gonçalves, proceedings of XXIX International Symposium on Multiparticle Dynamics (ISMD99), Providence, USA, August 9 -13, 1999

Figure Captions

Fig. (1) The rapidity distribution of particles produced in nucleus collisions at the same incident energy.

Fig. (2) The multiplicity multiplication factor in nucleus-nucleus collisions in terms of the yield in pp collision at the same incident energy. The p-S collision is represented by the black- plus line, S-S (crossed), S- Ag (triangle) and S-Au (circles).

Fig. (3) The multiplicity multiplication factor in nucleus-nucleus collisions in terms of the yield in p-S collision at the same incident energy. The black- plus line represents the S-S collision, S-Ag (crossed) and S-Au (triangles).

Fig. (4) The scaled rapidity distribution produced from the nucleus- nucleus collisions at the same incident energy.

Fig. (5) A tree diagram for the multi-peripheral process, producing n- particles in the final state.

Fig. (6) The particle rapidity distribution produced in p-S at multiple order collisions as predicted by the MPM.

Fig. (7) The particle rapidity distribution produced in p-S collision at 200 GeV incident proton energy as predicted by the MPM and compared with the experimental data SLAC-NA-035.

Fig. (8) The particle rapidity distribution produced in S-S at multiple order collisions as predicted by the MPM.

Fig. (9) The particle rapidity distribution produced in S-S collision at 200 GeV incident proton energy as predicted by the MPM and compared with the experimental data SLAC-NA-035.

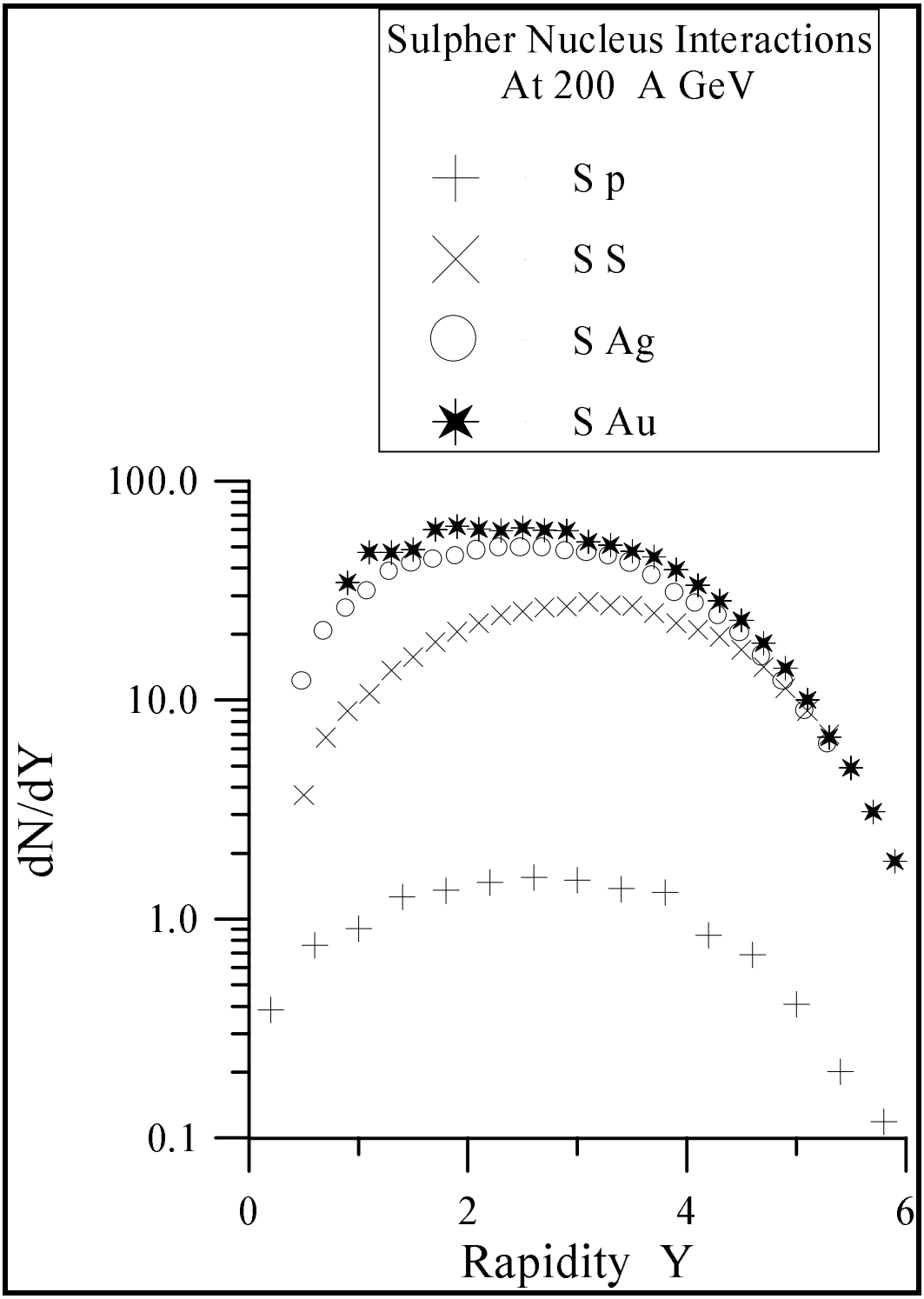
Sulpher Nucleus Interactions
At 200 A GeV
S p
S S
S Ag
S Au
100.0
10.0
1.0
0.1
dN/dY
0
2
4
6
Rapidity Y

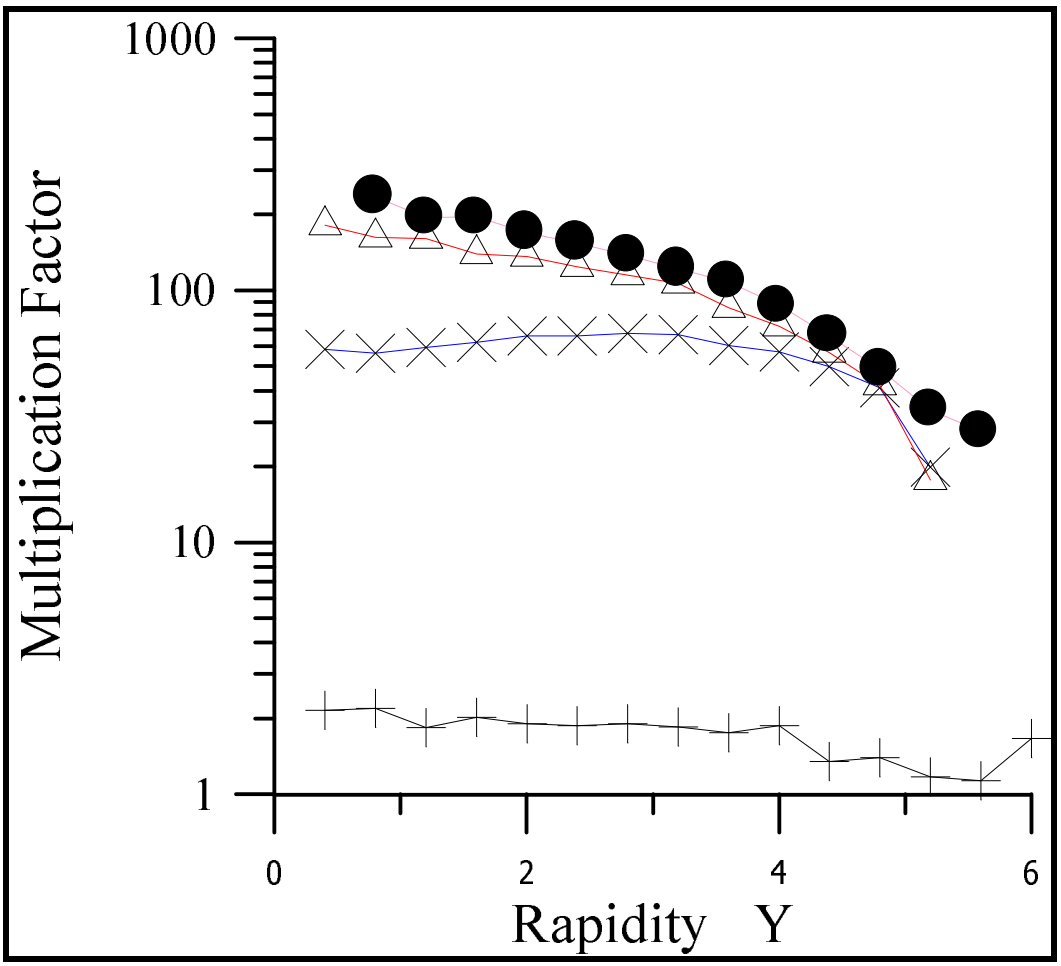
1000
100
10
1
Multiplication Factor
0
2
4
6
Rapidity Y

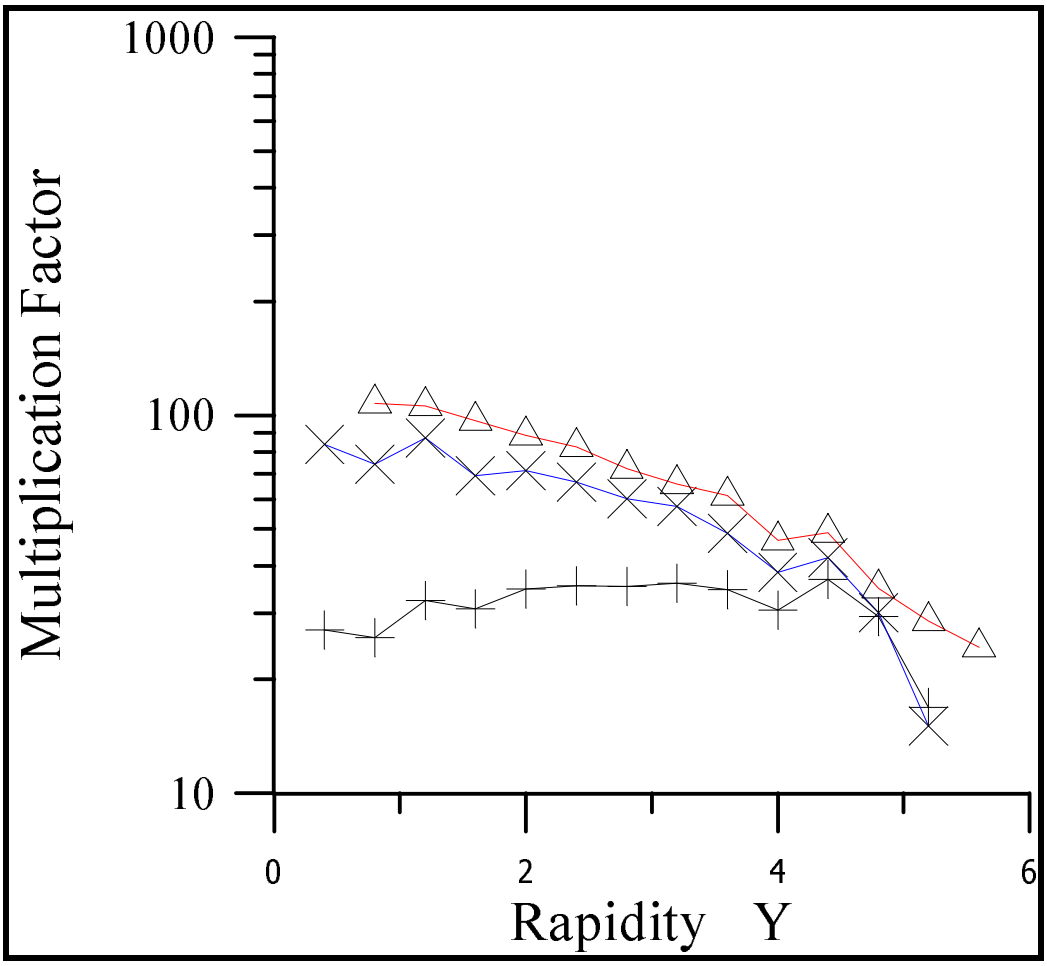
1000
100
10
Multiplication Factor
0
2
4
6
Rapidity Y

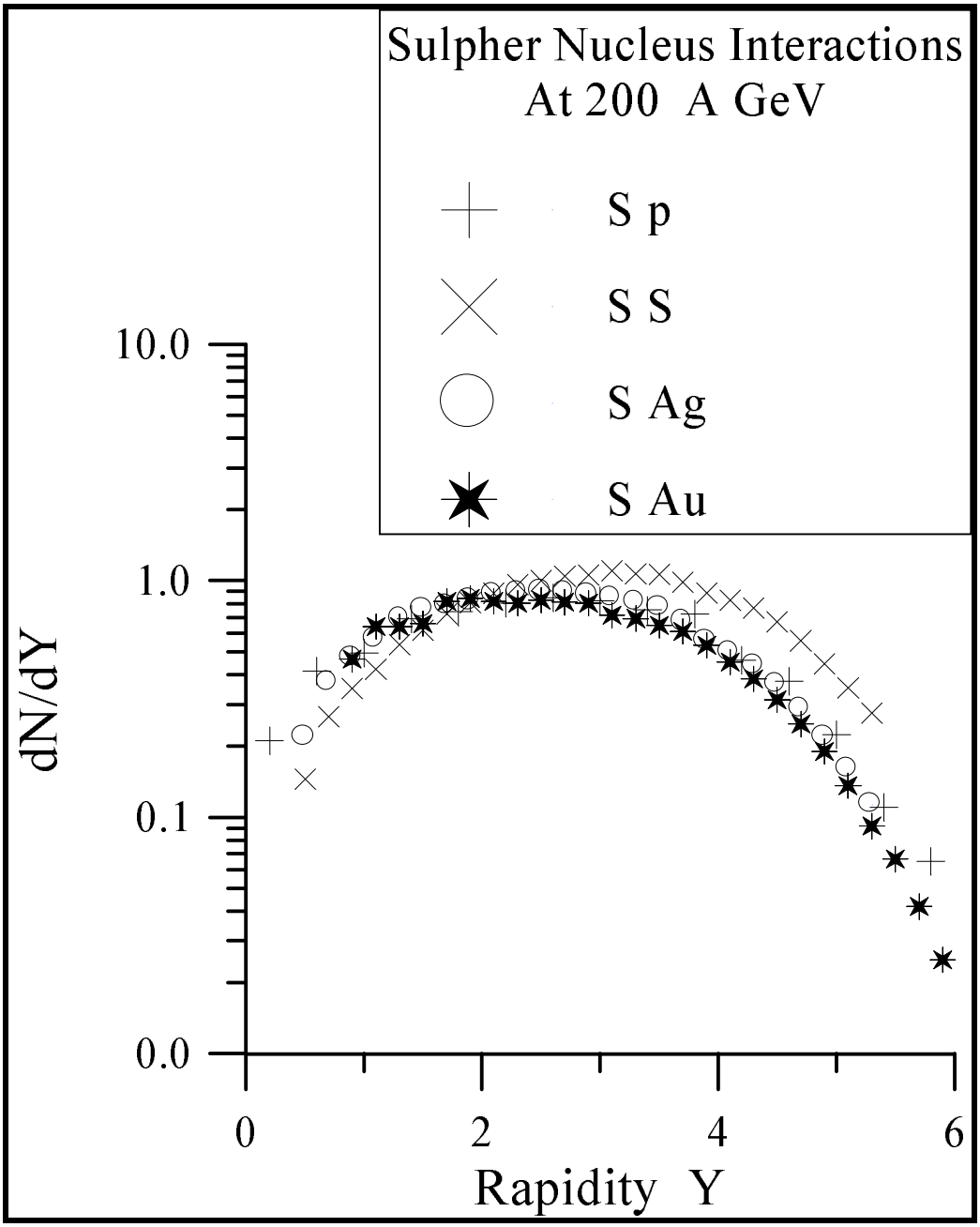
Sulpher Nucleus Interactions
At 200 A GeV
S p
S S
S Ag
S Au
10.0
1.0
0.1
0.0
dN/dY
0
2
4
6
Rapidity Y

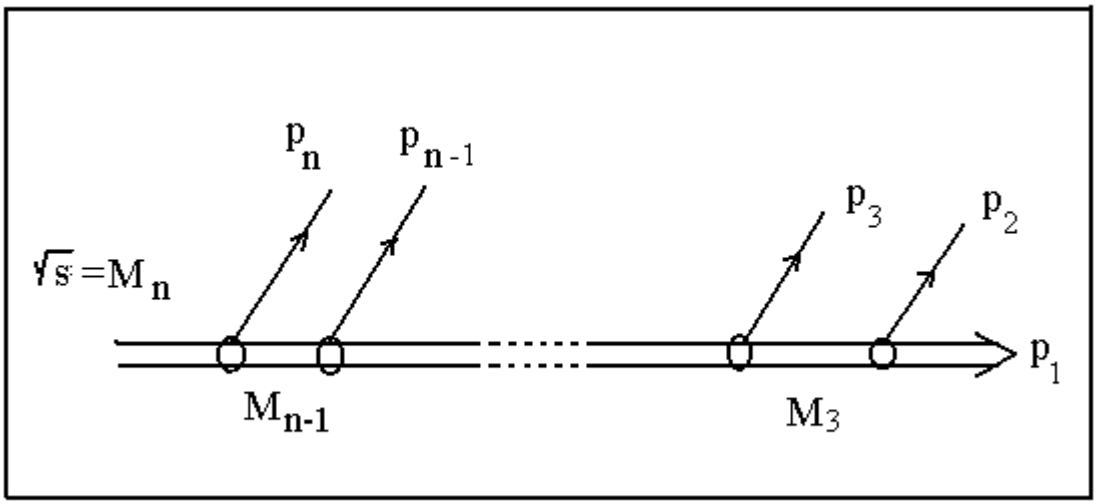
p_n
p_{n-1}
p_3
p_2
$\sqrt{s} = M_n$
p_1
M_{n-1}
M_3

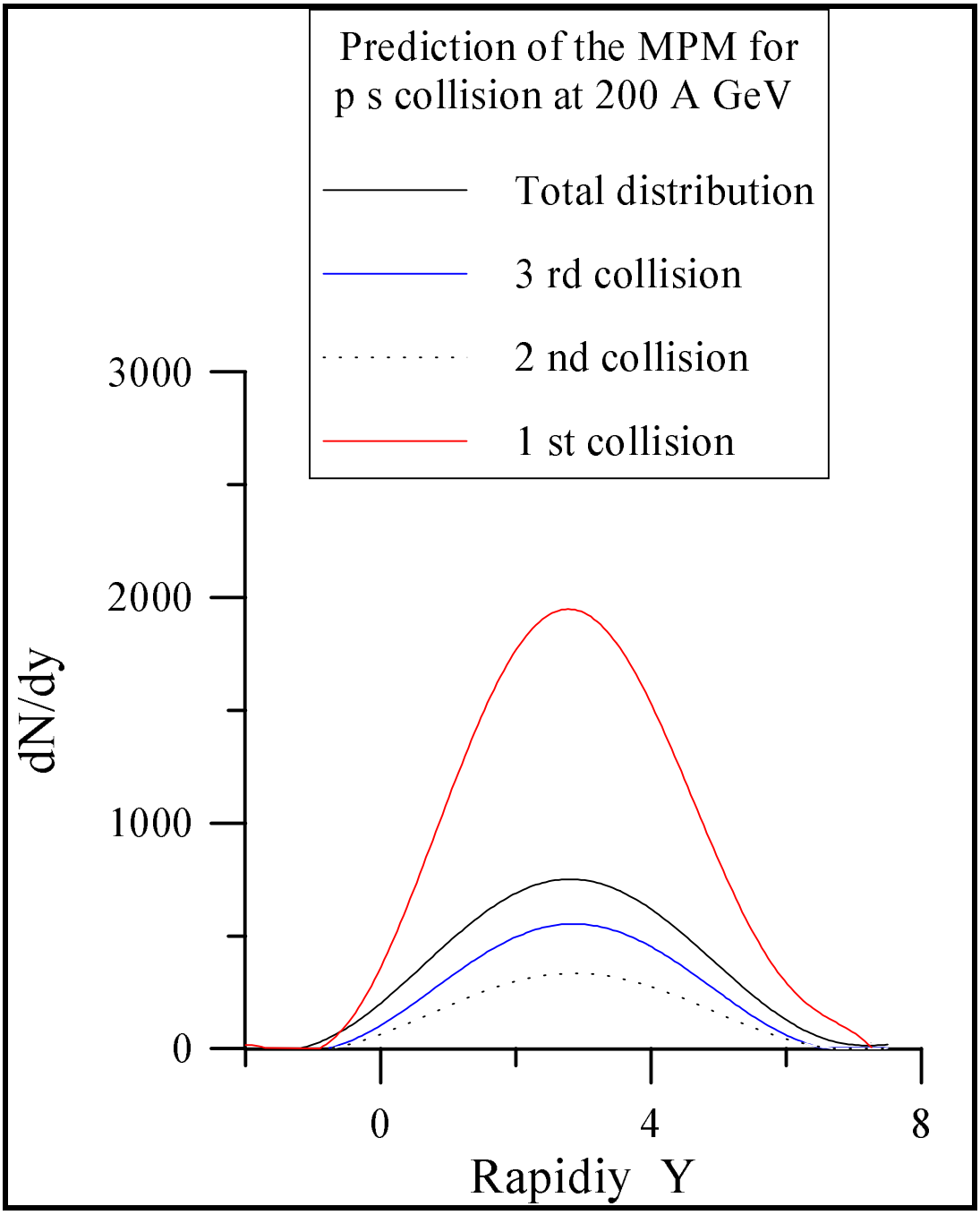
Prediction of the MPM for
p s collision at 200 A GeV
Total distribution
3 rd collision
2 nd collision
1 st collision
3000
2000
1000
0
dN/dy
0
4
8
Rapidiy Y

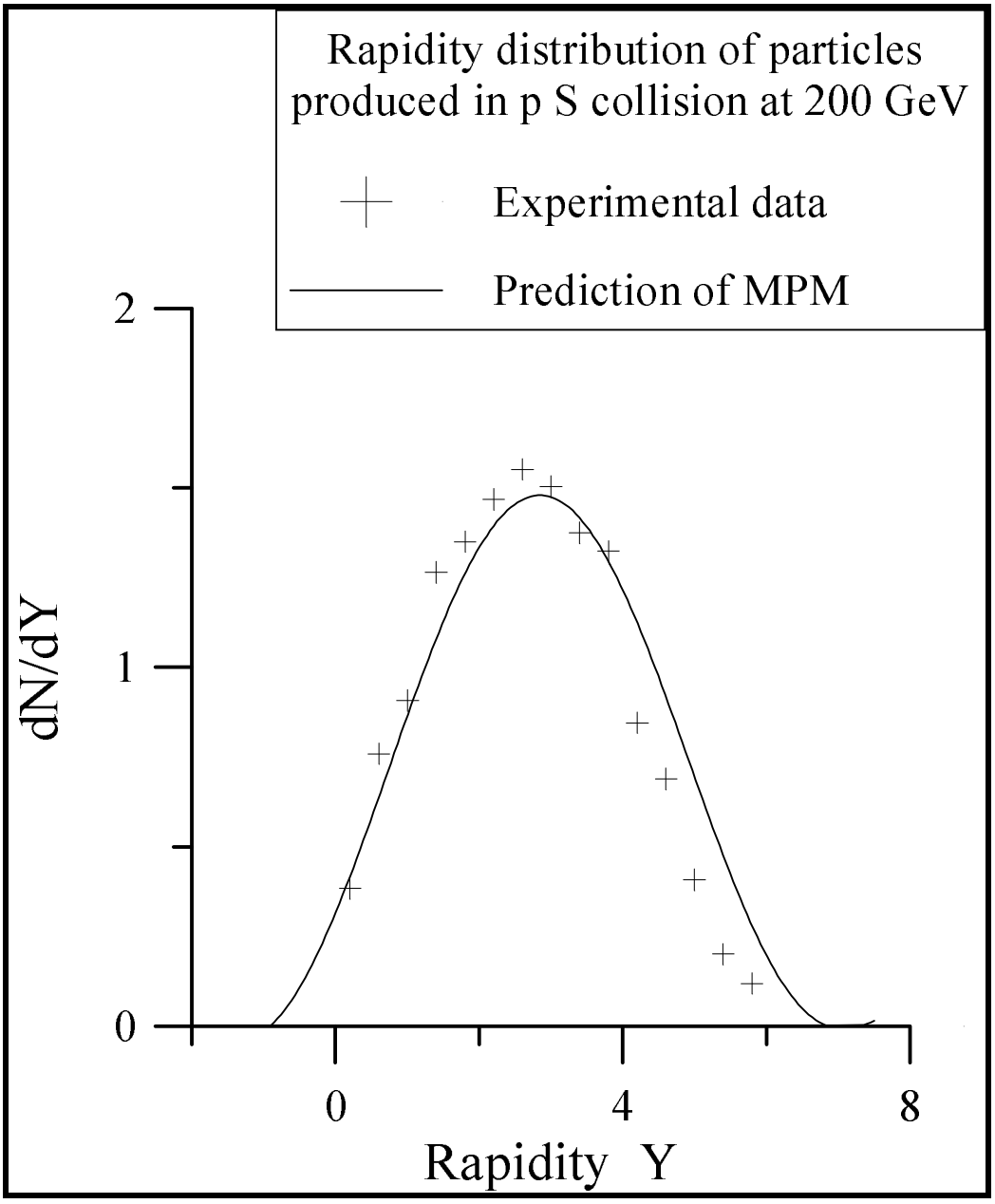
Rapidity distribution of particles
produced in p S collision at 200 GeV
Experimental data
Prediction of MPM
dN/dY
2
1
0
0
4
8
Rapidity Y

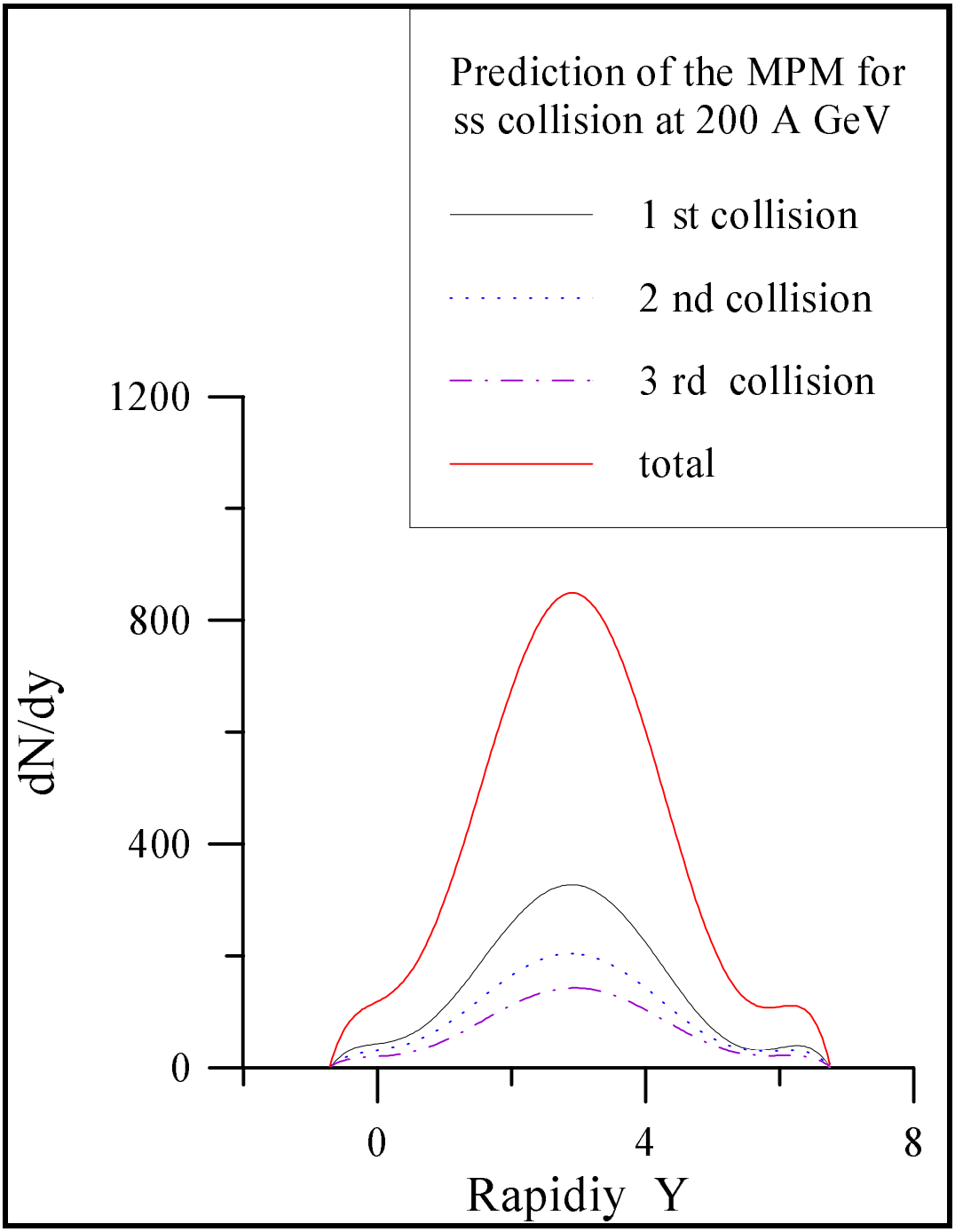
Prediction of the MPM for
ss collision at 200 A GeV
1 st collision
2 nd collision
3 rd collision
total
1200
800
400
0
dN/dy
0
4
8
Rapidiy Y

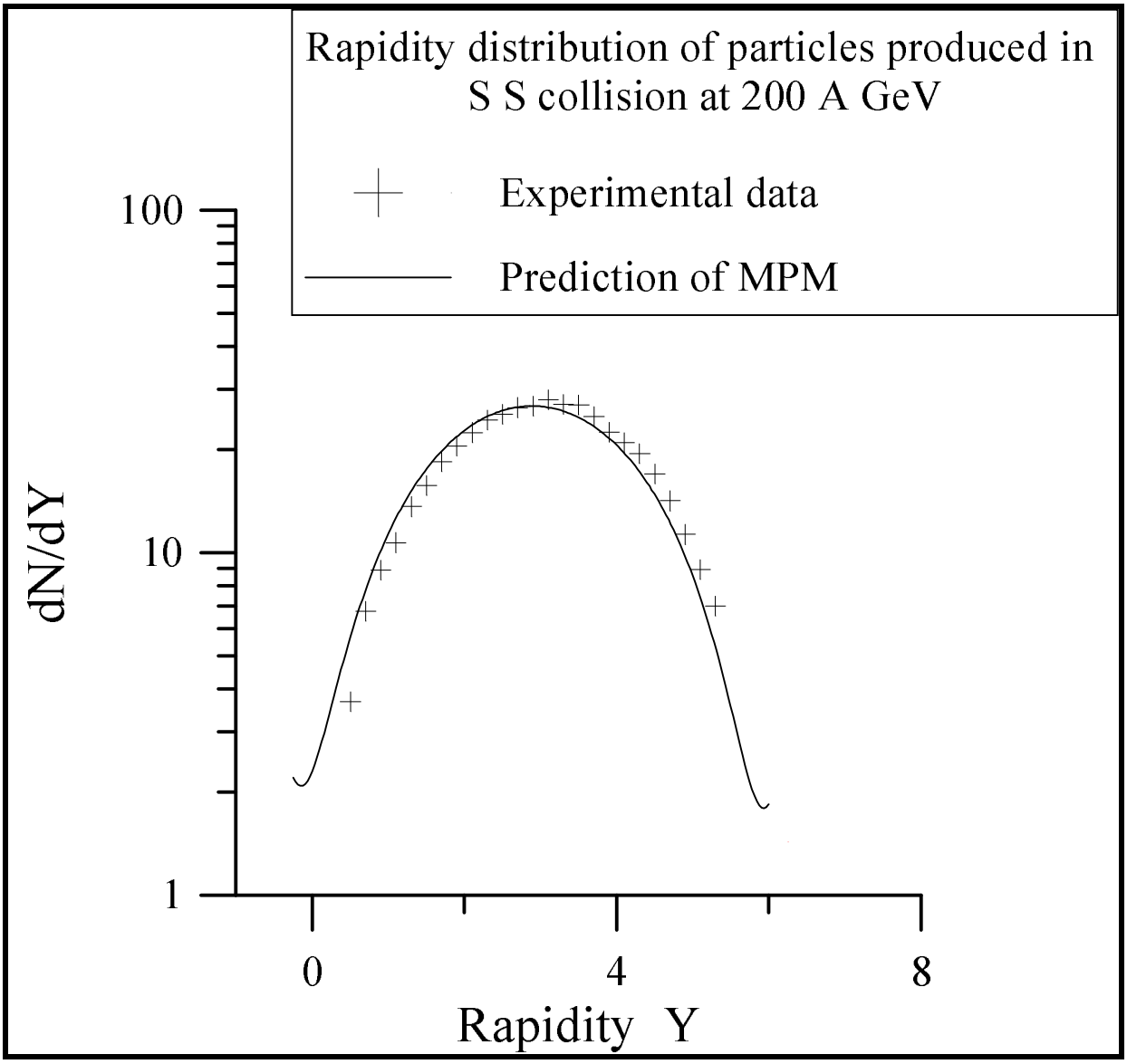
Rapidity distribution of particles produced in
S S collision at 200 A GeV
Experimental data
Prediction of MPM
100
10
1
dN/dY
0
4
8
Rapidity Y